Crystallization and Structure Formation in Polymer Blends with Strong Intermolecular Interactions: Blends of Poly(ethylene oxide) and Styrene-Hydroxystyrene Copolymers

Jaedong Cho,[1] Ruijian Xu,[1] Fengji Yeh,[2] Benjamin S. Hsiao,[2] James Runt[1]*

[1]Department of Materials Science and Engineering and Materials Research Institute, The Pennsylvania State University, University Park, PA 16802 USA
[2]Department of Chemistry, State University of New York, Stony Brook, NY 11794 USA

Summary: Time-resolved synchrotron wide- and small-angle X-ray scattering experiments were used to investigate crystallization behavior and microstructure development of a nearly monodisperse poly(ethylene oxide) [PEO] (M_w = 53,500), and its melt-miscible blends with two fractionated styrene – hydroxystyrene random copolymers [SHS]. PEO crystallization rates decrease significantly in the presence of the melt-miscible SHS copolymers. All low and high molecular weight SHS blends exhibit a crystallization process at relatively short times characterized by large Avrami exponents (n), followed by a dominant process with n near that of neat PEO. A model for the crystallization of these blends is proposed.

Keywords: crystallization, poly(ethylene oxide), polymer blends, SAXS, WAXD

Introduction

In order to gain greater insight into the influence of blending on crystallization and lamellar organization, we have undertaken a series of experimental studies on polymer blends containing poly(ethylene oxide) [PEO].[1,2,3] For example, time-resolved synchrotron wide- (WAXD) and small-angle X-ray scattering (SAXS) experiments were conducted to investigate the crystallization behavior and microstructure development of PEO and several melt-miscible PEO blends.[3] Blends were prepared with both weakly-interacting poly(methyl methacrylate), and two copolymers that exhibit relatively strong intermolecular interactions with PEO. However, it was difficult to assign specific origins to the different stages of the crystallinity – time behavior of the blends because of uncertainty due to the possible effects of PEO molecular weight fractionation, and contributions from fractionation and/or segregation of polymer diluent molecules. In an attempt to simplify the behavior and facilitate interpretation, the current paper

 DOI: 10.1002/masy.200350804

summarizes our investigation of crystallization and microstructure development in PEO blends, but this time using a narrow PEO molecular weight fraction and two fractionated samples of one of the strongly-interacting random copolymers used in our previous experiments.

Experimental

The PEO molecular weight fraction used in this study was purchased from Polymer Source Inc. and has a weight average molecular weight (M_w) of 53,500 and M_w/M_n = 1.07. Two representative 'fractions' of a 50/50 random copolymer of styrene and hydroxystyrene (SHS) were selected for these experiments. The higher molecular weight sample (HMW-SHS) was determined to have a somewhat lower SHS content (44 wt %) and an apparent weight average molecular weight of 72,700 (M_w/M_n = 2.1). This molecular weight was determined using GPC with dimethylformamide - 0.05 M LiBr as the mobile phase. Molecular weights are relative to PEO standards. The lower molecular weight SHS fraction (LMW-SHS) contained 50 wt % styrene and has an apparent M_w = 31,700 (M_w/M_n = 1.5). T_gs for the LWM- and HMW-SHS were determined by differential scanning calorimetry (DSC) to be ~ 150 °C.

PEO/SHS blends were prepared from 2 wt % solutions of 50/50 (w/w) THF/CH_2Cl_2. Films were cast on glass slides and dried in air at room temperature for 48 h and then under vacuum at 90 °C for 6 h. The dried films were then pressed at 69 MPa and 100 °C for 3 min and rapidly cooled in air to room temperature. PEO films were prepared by pressing powdery PEO under the same conditions as the blends. Samples were deposited into a small copper cell for time-resolved experiments.

Time-resolved simultaneous WAXD/SAXS experiments were conducted at the U.S. National Synchrotron Light Source, Brookhaven National Laboratory on the Advanced Polymers Beamline, X27C. The X-ray wavelength (λ) was 0.1309 nm and pinhole collimation was utilized. For SAXS, the sample-to-detector distance was 1.509 m, covering an angular range up to q ~ 1.0 nm^{-1} ($q = \frac{4\pi}{\lambda}\sin(\theta/2)$ and θ is the scattering angle). The WAXD 2θ range was ~8° to 40°, relative to λ = 0.154 nm. The scattering patterns from a duck tendon and a Lupolen polyethylene standard were used to calibrate the SAXS and WAXD detectors, respectively.

The real-time WAXD/SAXS experiments were conducted using a specially designed sample holder to facilitate a rapid jump between the melt temperature and selected T_cs. All samples were maintained for 5 min in the melt chamber before transferring to the crystallization chamber. SAXS data were first smoothed using a moving window averaging procedure, then background scattering due to thermal density fluctuations was subtracted using the procedure described in ref 4. Crystalline and amorphous layer thicknesses within lamellar stacks were determined using the calculated one-dimensional correlation function, $\gamma(r)$.[5] The relative invariant (Q) was obtained as the ordinate of the linear fit to the self-correlation portion of the correlation function. Defining B as the value of the abscissa where the ordinate first equals zero in $\gamma(r)$, and obtaining the long period (L) from the first maximum of $\gamma(r)$, $x_c(1 - x_c) = B/L$, where x_c is the linear crystallinity. Although one cannot apriori distinguish x_c from x_a (= 1 – x_c), it was shown in our earlier work that x_c for a polydisperse PEO was greater than 0.7.[1] Since the PEO under consideration here has lower average molecular weight, lamellar thicknesses for the strongly-interacting blends are greater than those of PEO at the same T_c, and SHS was found previously to reside primarily outside of lamellar stacks,[1] the larger of the two values of x_i for these blends can confidently be taken as x_c. The average lamellar thickness is then calculated from: $l_c = x_c \cdot L$. Likewise, the average amorphous layer thickness (l_a) within lamellar stacks is obtained from: $l_a = (1 - x_c) \cdot L$. Degrees of crystallinity were determined from the WAXD data using a curve fitting program in which a given diffraction profile was separated into three crystalline PEO reflections and an amorphous halo, assuming Gaussian profiles. The apparent degree of crystallinity was defined as the ratio of the area under the resolved crystalline peaks to the total area.

Results and Discussion

1 Poly(ethylene oxide)

Development of the crystallinity and lamellar microstructure of the 53.5K PEO fraction was followed at three crystallization temperatures (T_c): 45, 48 and 52 °C. No systematic changes in the positions of the WAXD crystalline reflections or widths at half peak height were detected during crystallization of either neat PEO or PEO in blends with SHS.

We observe a second order SAXS reflection for PEO crystallized at all T_cs, indicative of the development of relatively well-ordered lamellar stacks. For all PEO samples, the development of the SAXS invariant during crystallization generally mirrors that of the WAXD crystallinity. However, Q is found to consistently develop prior to the appearance of WAXD diffraction peaks, an observation common to many crystallizing polymer systems. The origin of this remains unclear: it has been variously associated with spinodal decomposition,[6] relative detector sensitivities,[7] and primary nucleation.[8]

PEO crystallization data are presented in in Figure 1. The Avrami equation can be written as:[9]

$$1- X_c = \exp(-zt^n) \qquad (1)$$

where X_c is the fraction of the final crystallinity developed up to time t, z is a function of the nucleation and growth rates, and n is in principle related to the growth geometry and type of nucleation. Although there is some noise in the data, the Avrami plots for PEO crystallized at all three temperatures up to $X_c \sim 92\%$, are best fit by single values of z and n (see Table 1). This is in contrast to our earlier research on polydisperse PEO in which we observed a distinct transition to a second process (having $n \sim 1$) in the vicinity of $X_c \sim 0.6 - 0.7$.[3] The current results confirm that this longer time process originates from molecular weight fraction during crystallization.[10] Fitted Avrami exponents for the three samples range from 2.6 to 3.8, more or less consistent with spherulitic crystallization (the latter observed in optical microscopy experiments).

Long period and lamellar thickness are frequently observed to decrease early in the crystallization process in time-resolved SAXS experiments of polymer crystallization.[e.g.3,11,12] Such behavior is often associated with crystallization ('insertion') of new lamella in amorphous regions between or within lamellae stacks.[e.g.13,14] Crystallization is rapid at 45 and 48 °C for the 53.5K PEO and the SAXS signal-to-noise ratio is low at short crystallization times (t_c), leading to uncertainty in the analysis of $\gamma(r)$. However, reliable correlation functions can be calculated over the course of crystallization at $T_c = 52$ °C. Both l_c and l_a decrease by ~2 nm with increasing time, becoming constant at longer t_c, consistent with the idea of crystallization of subsidiary lamellae (with restricted lamellar thickness) in non-crystalline regions between dominant lamellae. As expected for homopolymers, l_c and the long period at the conclusion of crystallization increase with

increasing T_c (from 17.4 to 20.5 nm, and 23 to28.2 nm, respectively) and the values compare favorably to those determined in our previously experiments on unfractionated PEO.[1,3]

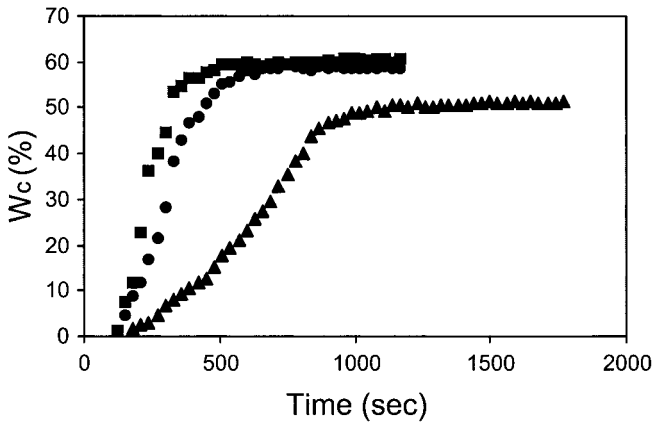

Fig. 1: Development of WAXD crystallinity for PEO as a function of crystallization time at 45 (■), 48 (●) and 52 °C (▲).

Table 1. Avrami parameters and final bulk crystallinities for PEO fractions.

T_c (°C)	$t_{1/2}$ (sec)[a]	W_c (%)	n	z
45	255	68	3.8	3.1×10^{-12}
48	310	62	2.9	7.4×10^{-3}
52	630	54	2.6	5.0×10^{-8}

[a] crystallization half-time

2 PEO/SHS Blends: LMW-SHS

The crystallization behavior of PEO/LMW-SHS blends at T_c = 45 and 48 °C was found to be very similar, and for the sake of brevity only the WAXD results for crystallization at 48 °C will be presented. Bulk crystallization rates for all SHS blends are considerably slower than PEO.

Representative Avrami plots are displayed in Figure 2 and fit parameters in Table 2. In addition to the role of SHS as a miscible polymeric diluent, this arises from a significant reduction in the equilibrium melting point (T_m^0) of PEO in the presence of SHS, due to their relatively strong intermolecular hydrogen bonding.[1] At a given T_c, crystallization proceeds at a significantly smaller degree of supercooling, ΔT, for the SHS blends, compared to neat PEO.

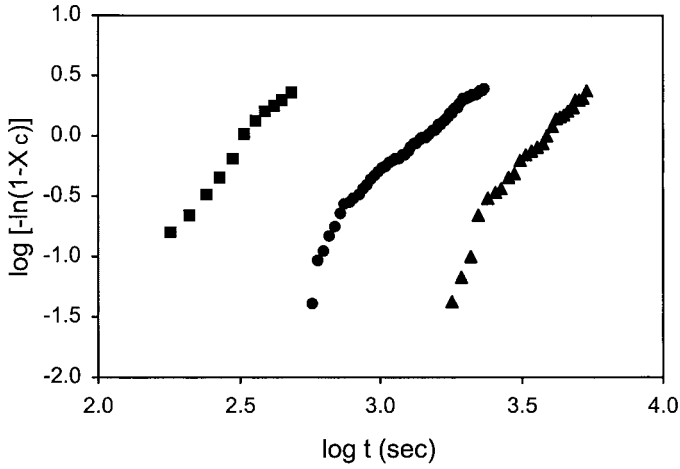

Fig. 2: Avrami plots for PEO and PEO/LMW-SHS blends at T_c = 48 °C. PEO (■), 90/10 LMW-SHS blend (●) and 80/20 LMW-SHS (▲).

The crystallization behavior of the SHS/PEO blends is more complex than that of the neat PEO fraction, even when containing only 10% SHS. As seen in Figure 2, 90/10 and 80/20 LMW-SHS blends appear to exhibit a relatively short time process (through ~20 - 25 % relative crystallinity) with a large apparent *n* (~6 - 7), similar to our previous findings on blends prepared with polydisperse PEO and SHS.[3] Although these large exponents are determined by only a modest number of data points, we consistently observe the same behavior for SHS blends with unfractionated or fractionated PEOs. In fact, similar behavior is observed in DSC studies of crystallization of these same blends.[15] Large Avrami exponents have been predicted for 3D crystallization of branched sheaf-like structures.[16,17] For all SHS blends, the first process is followed by a second dominant one having a 'more typical' Avrami exponent in the range of 2.0 – 2.6. The early time process has no counterpart in the behavior of fractionated (or

unfractionated) PEO, crystallized at this or any other T_c investigated, and seems to be uniquely associated with the influence of the polymeric diluent on the crystallization process.

Table 2. Avrami parameters for PEO/LMW-SHS blends crystallized at 48 °C.

Composition	$t_{1/2}$ (s)	W_c (%)	$X_{c,s}$ [a](%)	n	z
PEO	310	62	-	2.9	7.4×10^{-3}
90/10 SHS	1190	54	24	6.3	2.2×10^{-20}
				2.0	6.2×10^{-7}
80/20 SHS	3270	48	20	7.2	1.8×10^{-25}
				2.6	3.9×10^{-10}

[a] relative crystallinity at the end of the initial process

The crystallization time dependence of the SAXS microstructural parameters for SHS blends with <20% LMW-SHS (crystallized at 45 and 48 °C) is similar to that of PEO. However, blends containing 20% LMW-SHS, crystallized at 45 and 48 °C, exhibit a relatively large drop in L and l_c early in the crystallization process: L and l_c both decrease by 5 – 10 nm. An example of this behavior is provided in Figure 3. Some SHS chains become trapped in interlamellar regions, and we have shown previously that the remainder resides between stacks/fibrils.[1] This large drop in L and l_c early in crystallinity development is similar to the behavior we observed previously for polydisperse PEO blends with PMMA and SHS blends.[3] There is a close relationship between the crossover time from high *n* to more typical *n* values in the Avrami plots, and the time at which L and l_c become time independent.

Based on the results of the time-resolved WAXD/SAXS studies of blends with fractionated and polydisperse polymers, we propose the following model for crystallization of PEO/SHS blends. Early in crystallization, the process is envisioned as occurring via growth of lamellar stacks organized into a branched sheaf-like structure (that is, one with large *n*). Booth and Hay estimated that *n* can be as high as 14 for a highly branched structure.[17] As crystallization proceeds, growth of subsidiary stacks in uncrystallized regions between primary stacks seems likely.[18] To be

consistent with the experimental data, crystallization of secondary lamellar stacks must occur with restricted lamellar thickness (and long period) leading to a reduction in mean L and l_c, as observed experimentally. Smaller l_c in regions expected to be enriched in SHS seems at first to be counterintuitive, but could result from restricted lamellar thickening during formation of stable lamellae.[19] At longer times, L and l_c reach a plateau, and we speculate that crystallization of secondary stacks approaches the superstructure boundary. This would lead to a return to a 'normal' Avrami exponent for the remainder of the primary crystallization process.[16]

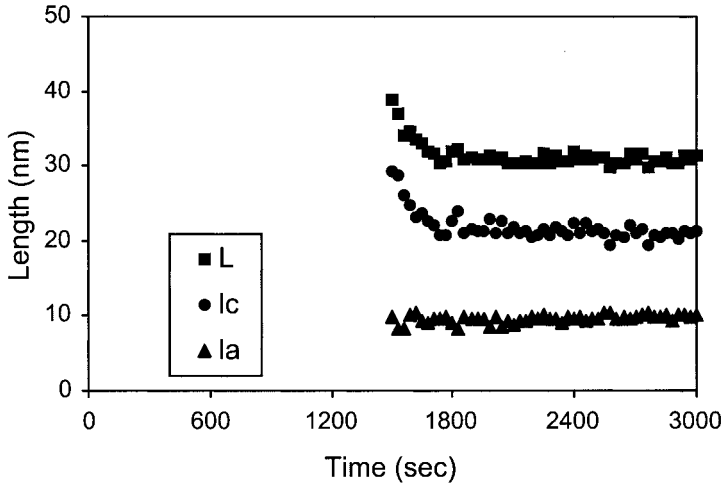

Fig. 3: Dependence of microstructural parameters on crystallization time for the 20 % LMW-SHS/PEO blend crystallized at 45 °C.

Table 3 provides a summary of L, l_c and l_a at the end of the time-resolved experiments for PEO and PEO/LMW-SHS blends crystallized at 45 and 48 °C. In general, the increase in long period results from both an increase in l_a, due to SHS chains trapped in interlamellar regions, and an increase in l_c due to a reduction in ΔT resulting from the presence of the strongly-interacting SHS. The former conclusion is in line with the significantly larger invariant observed for the blends in static SAXS experiments compared to that of neat PEO (SHS has an electron density of 0.573 vs.

0.612 mol e/cc for amorphous PEO).[20] Based on the experimental values for l_c we estimate that the equilibrium melting point is depressed by ~5 °C for the 20 % SHS blend, the same as estimated for 20% blends of polydisperse PEO and SHS.[1] The increase in l_a with SHS content is significantly higher than observed previously for comparable polydisperse blends. This is likely a consequence of more rapid crystallization of the blends in this study compared to the polydisperse PEO/SHS blends, trapping more SHS in interlamellar regions in the present case.

Table 3. Microstructural parameters for PEO and PEO/LMW-SHS blends at the conclusion of time-resolved experiments.

Composition	T_c (°C)	L (nm)	l_c (nm)	l_a (nm)
PEO	45	23.0	17.4	5.6
	48	26.2	20.7	5.5
90/10 SHS	45	26.2	19.3	6.9
	48	28.8	20.8	8.0
85/15	45	28.0	19.3	8.7
	48	30.5	20.8	9.7
80/20	45	31.5	21.3	10.2
	48	34.1	22.4	11.7

3 PEO/SHS Blends: HMW-SHS

Like the LMW-SHS/PEO blends, the behavior at T_c = 48 °C is nearly the same for the HMW-SHS/PEO blends crystallized at 45 °C, and only the former is discussed here. The crystallization behavior is very similar to that of the LMW-SHS blends: a first process with large apparent *n*, followed by a second dominant process with Avrami exponent similar to that of the neat PEO. Overall crystallization rates are significantly faster for 90/10 HMW-SHS than the comparable LMW-SHS blends. This is likely a consequence of higher mobility and segregation length scale of LMW-SHS, and relative accumulation of LMW-SHS in the uncrystallized phase, inhibiting

crystallization. This is also in keeping with the higher degrees of crystallinity observed for 90/10 HMW-SHS blends at the conclusion of the time-resolved experiments. In contrast, however, overall crystallization rates and degrees of crystallinity are comparable for the much more slowly crystallizing 80/20 LMW- and HMW-SHS blends. This implies that crystal growth has been slowed sufficiently (relative to SHS diffusion) so that it dominates the determination of the impurity segregation length scale.

The microstructure parameters at the conclusion of the SAXS experiments are quite similar for the low and high molecular weight SHS blends (see Table 4 for a summary of the PEO/HMW-SHS blend data), implying the same reduction in T_m^0 for the two SHS copolymers. In addition, the crystallization time dependence of the microstructural parameters for the HMW- and LMW-SHS blends is similar.

Table 4. Microstructure parameters for PEO and PEO/HMW-SHS blends at the conclusion of time-resolved experiments.

Composition	T_c (°C)	L (nm)	l_c (nm)	l_a (nm)
PEO	45	23.0	17.4	5.6
	48	26.2	20.7	5.5
90/10 SHS	45	25.6	18.8	6.8
	48	27.6	19.6	8.0
80/20	45	30.9	21.8	9.1
	48	36.7	25.5	11.2

Conclusion

The WAXD crystallinity – time data for the 53.5K PEO molecular weight fraction, crystallized between 45 and 52 °C, are best fit by a single Avrami expression. This is in contrast to our earlier research on a polydisperse PEO in which a distinct transition to $n \sim 1$ behavior in the vicinity of $X_c \sim 0.6 - 0.7$ was observed.[3] The results in the present paper demonstrate that this longer term

process originates from molecular weight fractionation of the polydisperse PEO during crystallization.

PEO crystallization rates decrease significantly in the presence of the melt-miscible SHS copolymers. All LMW- and HMW-SHS/PEO blends exhibit a relatively short-time crystallization process characterized by large *n* values, followed by a dominant process with *n* near that of PEO. The magnitude of the initial decrease in mean L and l_c is significantly larger for blends containing either LMW- or HMW-SHS. In addition, the time at which L and l_c become time independent is similar to that at which the Avrami plots crossover from high *n* to more typical values. Our data leads us to propose that crystallization occurs initially by growth of lamellar stacks organized into a branched sheaf-like structure. As crystallization continues, growth of secondary lamella stacks in uncrystallized regions between primary stacks seems likely. To be consistent with the experimental data, crystallization of secondary stacks must occur with restricted lamellar thickness (and long period). At longer times, L and l_c become constant and crystallization of secondary stacks presumably approaches the superstructure boundary, leading to a typical Avrami exponent for the remainder of the primary crystallization process.

Acknowledgments

The Penn State authors would like to express their appreciation to the National Science Foundation, Polymers Program (DMR – 9900638 and – 0211056) for its support of this research. BH and FY thank a Department of Energy grant (DEFG0299ER45760) for support of the AP-PRT beamline.

[1] S. Talibuddin, L. Wu, J. Runt, J.S. Lin. *Macromolecules* **1996** *29*, 7527.
[2] L. Wu, M.S. Lisowski, S. Talibuddin, J. Runt. *Macromolecules* **1999**, *32*, 1576.
[3] M.S. Lisowski, Q. Liu, J.D. Cho, J. Runt, F. Yeh, B.S. Hsiao. *Macromolecules* **2000**, *33*, 4842.
[4] B.S. Hsiao, R.K. Verma. *J. Synchrontron Rad.* **1998**, *5*, 23.
[5] G.R. Strobl, M. Schneider. *J. Polym. Sci., Polym. Phys.* **1980**, *18*, 1343.
[6] P.D. Olmsted, W.C.K. Poon, T.C.B. McLeish, N.J. Terrill, A.J. Ryan. *Phys. Rev. Lett.* **1998**, *81*, 373.
[7] Z.-G.Wang, B.S. Hsiao, C. Kopp, E.B. Sirota, S. Srinivas. *Polymer* **2000**, *41*, 8825.
[8] E.-Q. Chen, X. Weng, A. Zhang, I. Mann, F.W. Harris, S.Z.D. Cheng, R. Stein, B.S. Hsiao, F. Yeh. *Macromol.Rapid Commun.* **2001**, *22*, 611.
[9] M.J. Avrami. *Chem. Phys.* **1939**, *7*, 1103.
[10] S.Z.D. Cheng, B. Wunderlich. *J. Polym. Sci. Polym. Phys.* **1986**, *24*, 595.
[11] R. Verma, H. Marand, B.S. Hsiao. *Macromolecules* **1996**, *29*, 7767.

[12] D.A. Ivanov, R. Legras, A.M. Jonas. *Macromolecules* **1999**, *32*, 1582.
[13] G. Dreezen, N. Mischenko, M.H.J. Koch, H. Reynaers, G. Groeninckx. *Macromolecules* **1999**, *32*, 4015.
[14] R. Kolb, C. Wutz, N. Stribeck, G. von Krosigk, C. Riekel. *Polymer* **2001**, *42*, 5257.
[15] M. Kanchanasopa, J. Runt. Unpublished results.
[16] B. Wunderlich. *Macromolecular Physics*. New York: Academic Press, **1976** (Vol. 2).
[17] A. Booth, J.N. Hay. *Brit. Polym. J.* **1972**, *4*, 9.
[18] F. Yeh, B.S. Hsiao, B. Chu, B.B. Sauer, E.A. Flexman. *J. Polym. Sci. Polym. Phys.* **1999**, *37*, 3115.
[19] J. Runt. *Macromolecules* **1981**, *14*, 420.
[20] J.D. Cho, J.T. Garrett, J.S. Lin, J. Runt. Manuscript in preparation.